# Simulation of a Particulate Flow in 3D Using Volume Penalization Methods

Philippe Angot[1], Léa Batteux[2(✉)], Jacques Laminie[2], and Pascal Poullet[2]

[1] Université d'Aix–Marseille, 13007 Marseille, France
[2] Université des Antilles, Campus de Fouillole, Pointe–à–Pitre 97157, Guadeloupe
lea.batteux@univ-antilles.fr

**Abstract.** We are concerned with modelling a particulate flow in a three-dimensional domain. The particles are assumed to be rigid, allowing us to describe their motion using the Newton laws. As we aim to take into account complex shapes for the solid inclusions, we adopt volume penalization methods. Those methods allow us to extend the fluid problem inside the solid domain by assimilating the particle as a porous medium. The homogeneous fluid flow is governed by the incompressible Navier-Stokes equations. The whole problem is solved with a projection-correction method using finite volumes and a staggered mesh to ensure the inf-sup condition for the stability. Regarding the transport of the particles, a marker-based front tracking method is used for the fluid-solid interface, as well as a collision strategy. Both penalization methods are studied and compared in the context of particulate flows.

**Keywords:** Fluid–structure interactions · Fictitious domain · Penalization

## 1 Introduction

We are interested in the modelling of fluid-solid systems where we consider rigid solid inclusions in an incompressible viscous fluid flow in a three-dimensional domain. Such problems led to a wide panel of methods to attempt to model and reproduce faithfully the fluid-solid interactions observed in real life problems. Depending on the needs, different degrees of coupling between the fluid and the particles may be applied. In what follows we will resort to a strong coupling to make evident the influence of the solid inclusions on the fluid. Using an Eulerian formulation for the fluid flow, we extend the fluid problem inside the solid domain as defined by the fictitious domain methods. Given the assumptions on the particles we require a rigidity constraint on the solid domain. Among the most famous methods in this field, the works of Glowinsky et al. [1] which resort to Lagrange multipliers for the constraint, and volume penalty methods [2,3]. The latter idea is based on porous laws and will be considered in our model.

The computational tests have been performed using the server of the Centre Commun de Calcul Intensif (C3I) of Université des Antilles.


M. Deville et al. (Eds.): TI 2018, NNFM 149, pp. 103–109, 2021.
https://doi.org/10.1007/978-3-030-65820-5_9

Let us introduce our physical domain $\Omega$ along with its boundary $\Gamma$, containing the fluid domain $\Omega_f(t)$ and $N$ particles $\Omega_s^i(t)$ such that $\cup_{i=1}^{N}\Omega_s^i(t) = \Omega_s(t)$ defines the solid domain. Therefore we have $\Omega_f(t) = \Omega \setminus \overline{\Omega_s(t)}$. Given the assumptions, we will work with the incompressible Navier-Stokes equations to govern the fluid flow,

$$
\begin{cases}
\rho\Big(\dfrac{\partial \boldsymbol{v}}{\partial t} + (\boldsymbol{v}\cdot\nabla)\,\boldsymbol{v}\Big) - 2\boldsymbol{\nabla}\cdot(\mu D(\boldsymbol{v})) + \nabla p = \boldsymbol{f} & \text{in} \quad \mathbb{R}^+ \times \Omega_f(t) \\
\boldsymbol{\nabla}\cdot\boldsymbol{v} \quad = 0 & \text{in} \quad \mathbb{R}^+ \times \Omega_f(t) \\
 & \\
\boldsymbol{v}(0,\boldsymbol{x}) = \boldsymbol{v}_0 & \text{in} \quad \mathbb{R}^+ \times \Omega_f(0) \\
\boldsymbol{v}(t,\boldsymbol{x}) = \boldsymbol{v}_\Gamma & \text{on} \quad \mathbb{R}^+ \times \Gamma \\
\boldsymbol{v}(t,\boldsymbol{x}) = \boldsymbol{V}_i(t) + \boldsymbol{\omega}_i(t) \times \boldsymbol{r}_i(t,\boldsymbol{x}) & \text{on} \quad \mathbb{R}^+ \times \partial\Omega_s^i(t)
\end{cases}
$$

with the fluid velocity $\boldsymbol{v}$ and pressure $p$ as the unknowns. The fluid here is defined by its density $\rho$ and dynamic viscosity $\mu$. The term $\boldsymbol{D}(\boldsymbol{v})$ in the momentum equation refers to the tensor of deformation rate of the fluid, and we have: $\boldsymbol{D}(\boldsymbol{v}) = \frac{1}{2}(\boldsymbol{\nabla v} + (\boldsymbol{\nabla v})^T)$. The last relation defines the no–slip condition; it closes the boundary conditions on $\Omega_f$ and enables the coupling with the solid domain. It states that the fluid velocity and the solid velocity are equal on the fluid–solid interface. Finally, as the particles are assumed to be rigid, their motion can be described using the translational and rotational velocities $(\boldsymbol{V}_i, \boldsymbol{\omega}_i)$ of their respective center of mass $\boldsymbol{X_i}$. As such we can define the rigid velocity field $\boldsymbol{v}_s(t,\boldsymbol{x})$ in $\Omega_s(t)$: $\forall \boldsymbol{x} \in \overline{\Omega_s(t)}$, $\exists(\boldsymbol{V}_i(t), \boldsymbol{\omega}_i(t))$, $\boldsymbol{v_s}(t) = \boldsymbol{V}_i(t) + \boldsymbol{\omega}_i(t) \times \boldsymbol{r}_i(t,\boldsymbol{x})$ where $\boldsymbol{r}_i(t,\boldsymbol{x}) = \boldsymbol{x} - \boldsymbol{X_i}(t)$. In addition we have for each particle that,

$$
\begin{cases}
M_i \dfrac{d\boldsymbol{V}_i}{\delta t} \quad = \displaystyle\int_{\Omega_s^i(t)} \rho_s \boldsymbol{f}_i(t,\boldsymbol{x}) dx + \int_{\partial\Omega_s^i} \boldsymbol{\sigma}(\boldsymbol{v},p)\cdot\boldsymbol{n} dS \\
\dfrac{d(J_i(t)\boldsymbol{\omega}_i)}{\delta t} = \displaystyle\int_{\Omega_s^i(t)} \rho_s \boldsymbol{r}_i(t,\boldsymbol{x}) \times \boldsymbol{f}_i(t,\boldsymbol{x}) dx + \int_{\partial\Omega_s^i} \boldsymbol{r}_i(t,\boldsymbol{x}) \times (\boldsymbol{\sigma}(\boldsymbol{v},p)\cdot\boldsymbol{n}) dS
\end{cases}
$$

Here the particle is subjected to the exterior force $\boldsymbol{f}_i$. The coupling with the fluid exists within the surface integrals, as they involve $\boldsymbol{\sigma}(\boldsymbol{v},p) = (-p\boldsymbol{I} + 2\mu\boldsymbol{D(v)})$, the surface stress tensor of the incompressible fluid. The surface integral applied to the translational (resp. rotational) acceleration will be denoted $\boldsymbol{F}_i$ (resp. $\boldsymbol{T}_i$). We also define the density, mass and inertia tensor $(\rho_s, M_i, J_i)$ of the particle $i$.

So as to prevent the use of time–dependent spatial meshes, we resort to fictitious domain methods to extend the fluid problem inside the solid domain. In our case we will be using and comparing the L2–penalty and the H1–penalty methods, which consist in penalizing specific quantities in the fluid problem. Convergence estimates can be found in [2,4] for fixed obstacles. Notably, the L2–penalty has a convergence rate of $\mathcal{O}(\eta^{1/2})$ in the fluid in regard to the penalization parameter $\eta$ whereas the H1–penalty has a convergence rate of $\mathcal{O}(\eta)$.

### 1.1 The Darcy or L2–Penalty

We penalize the velocity itself by introducing a perturbation term to the momentum equation in order to extend the problem inside the solid domain:

$$\begin{cases} \rho\Big(\dfrac{\partial \boldsymbol{v}}{\partial t} + (\boldsymbol{v}\cdot\nabla)\boldsymbol{v}\Big) - 2\boldsymbol{\nabla}\cdot(\mu D(\boldsymbol{v})) + \nabla p + \dfrac{\mu}{\eta}\mathbf{1}_{\Omega_s}(\boldsymbol{v}-\boldsymbol{v}_s) = \boldsymbol{f} & \text{in } \mathbb{R}^+\times\Omega \\ \boldsymbol{\nabla}\cdot\boldsymbol{v} = 0 & \text{in } \mathbb{R}^+\times\Omega \end{cases}$$

The parameter $\eta$ roughly describes the permeability of the solid domain, which is now considered as a porous medium. The latter will be taken as small as possible, in order to obtain the no–slip condition on $\partial\Omega_s$ in a weak sense with fixed point iterations regarding the convergence of $\boldsymbol{v}_s$.

Following the introduction, the system of equations above is coupled to the Newton laws for the transport of the solid domain. Owing to the modified momentum equation, we can consider for the fluid contributions on the particle $\Omega_s^i(t)$:

$$\begin{aligned} \boldsymbol{F}_i &= \lim_{\eta\to 0}\frac{\mu}{\eta}\int_{\Omega_s^i(t)}(\boldsymbol{v}-\boldsymbol{v}_s)dx + \rho\int_{\Omega_s^i(t)}\frac{d\boldsymbol{v}}{dt}dx \\ \boldsymbol{T}_i &= \lim_{\eta\to 0}\frac{\mu}{\eta}\int_{\Omega_s^i(t)}\boldsymbol{r}_i(t,\boldsymbol{x})\times(\boldsymbol{v}-\boldsymbol{v}_s)dx + \rho\int_{\Omega_s^i(t)}\boldsymbol{r}_i(t,\boldsymbol{x})\times\frac{d\boldsymbol{v}}{dt}dx \end{aligned}$$

Using these definitions, one deals with volume integrals, favoring greatly their computation in the context of fictitious domain methods.

### 1.2 The Viscous or H1–Penalty

We constraint the extended fluid velocity by penalizing its tensor of deformation rate $\boldsymbol{D}(\boldsymbol{v})$ inside the solid domain, in the momentum equation. To achieve this we resort to a multiphase flow representation of the problem, using the non–homogeneous incompressible Navier-Stokes equations with variable viscosity,

$$\begin{cases} \dfrac{\partial\rho}{\partial t} + \Big(\boldsymbol{v}\cdot\nabla\Big)\rho = 0 & \text{in } \mathbb{R}^+\times\Omega \\ \dfrac{\partial(\rho\boldsymbol{v})}{\partial t} + \boldsymbol{\nabla}\cdot(\rho\boldsymbol{v}\otimes\boldsymbol{v}) - 2\boldsymbol{\nabla}\cdot(\mu(\rho)D(\boldsymbol{v})) + \nabla p = \boldsymbol{f} & \text{in } \mathbb{R}^+\times\Omega \\ \boldsymbol{\nabla}\cdot\boldsymbol{v} = 0 & \text{in } \mathbb{R}^+\times\Omega \end{cases}$$

along with inflow boundary conditions for $\rho$ on $\{\boldsymbol{x}\in\Gamma, (\boldsymbol{v}(t,\boldsymbol{x})\cdot\boldsymbol{n}(\boldsymbol{x}))<0\}$ as well as initial conditions. Consequently we have introduced the transport equation of the two–valued density $\rho(t,\boldsymbol{x}) \geq \underline{\rho} > 0$, which will carry out the transport of the particles rather than the Newton laws. Similarly, we have for the viscosity: $\mu_f \leq \mu(\rho) \leq \mu_s$. The solid viscosity $\mu_s$ will be taken as great as possible to enforce the penalization of the tensor $\boldsymbol{D}(\boldsymbol{v})$. We aim that way to tend towards $\|\boldsymbol{D}(\boldsymbol{v})\|_{\boldsymbol{L}^2(\Omega_s(t))} = 0$. With this property we can go back to a rigid motion velocity field in $\Omega_s(t)$ for an accurate representation of the rigid behaviour of the particles.

## 2 Numerical Method to Solve the Problem

In the present section we describe time and spatial discretization schemes applied to the penalized problems, followed by the strategies regarding the fluid–structure coupling. We resort to the incremental projection scheme [5,6] adapted to both penalty methods to solve the extended problem in $\Omega$. Using the Hodge–Helmholtz decomposition of a given vector in $\boldsymbol{L}^2(\Omega)$, we are able to decouple the computation of the velocity and pressure. In a first sub-step we account for the viscous terms to determine a predicted velocity, followed by a second sub-step where we enforce the incompressibility constraint to obtain the pressure and corrected velocity. For the discretization of the derivatives, we use a BDF2 formulation for the time derivative of the velocity and a Richardson extrapolation for the non—linear inertia term. Thereafter we complete the projection scheme with the transport of the solid domain. For the Darcy penalty, we use an implicit scheme of the Newton laws in regards to the particle velocities.

Resorting to an advection scheme of the phase field of the particles for the viscous penalty could render difficult the localisation of the fluid–solid interface. Instead we carry out the transport of markers defined on the surface of the particles using Runge–Kutta schemes [7]. We require at least $N_{df} = 6$ markers for each particle, $N_{df}$ being the degree of freedom for a 3–dimensional rigid solid. Using the no–slip condition, we end up with at most an overdetermined system given by the rigid–body equations valued on each marker.

As we aim to simulate a large collection of particles we need to adopt a fitting strategy to account for the potential collisions between particles or the boundaries of the computational domain. One can resort to repulsive forces using the given position and orientation of the particle. In our case we will couple the fluid–solid scheme above with the method introduced in [8]. In the latter reference we break down a particle in sub–spheres in such a way that we can define the particle as the union of the convex hulls of two neighbouring sub–spheres (Fig. 1). Using an Uzawa algorithm, the predicted velocities of all sub–spheres are projected on a set of admissible velocities.

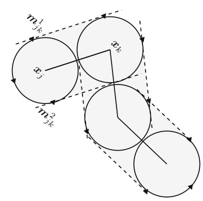

**Fig. 1.** Defining the markers for a particle in 2D

Regarding the spatial discretizations, finite volumes and a staggered mesh have been chosen. We define the fields for the penalty quantities $(\rho, \mu, \mathbf{1}_{\Omega_s})$ on the velocity grids. To compute those fields on the cells where the fluid-solid interface is located, we adopt an averaging method.

# 3 Validation Tests and Comparisons

## 3.1 Dropping a Ball in a Viscous Fluid

For a first test we drop a rigid heavy sphere in a viscous fluid and observe it attaining its terminal velocity according to the principle that the drag force exerted on the particle by the fluid as well as buoyancy balances the gravity applied to the sphere. We define the fluid using the density $\rho_f = 1$ and viscosity $\mu_f = 0.01$. The sphere with radius $r = 0.05$ and density $\rho_s = 5$ is falling in the rectangular domain $[0,1] \times [0,1] \times [0,3]$ to which we applied channel–flow boundary conditions. The gravity constant applied to the ball is $g = 98.1$. We take for the penalty parameters $\mu_s = 10^4$ and $1/\eta = 10^7$. For the time step we will be using $\delta t = 0.001$. The spatial step $h$ is such that $h = \max_{i=x,y,z} h_i = 1/50$. The initial position for the ball is $(0.5, 0.5, 1)$ (Figs. 2 and 3).

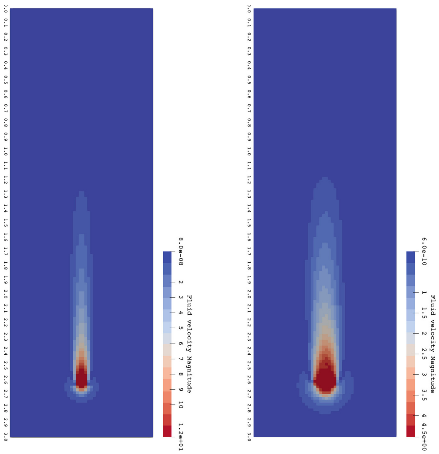

**Fig. 2.** Fluid velocity magnitude for the L2–penalty (left) and H1–penalty (right) when $Z(t) = 2.617$

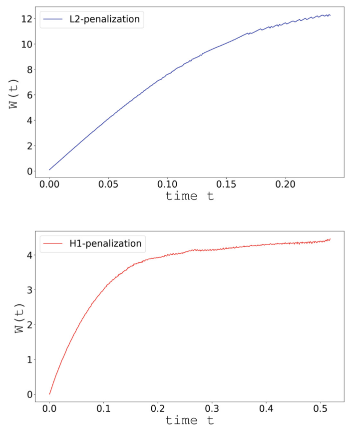


**Fig. 3.** $W$-component of the translational velocity reaching a terminal velocity of the for the L2–penalty (above) and H1–penalty (bottom)

In both cases the velocity of the particle keeps a straight trajectory and reaches a terminal velocity, which is a first satisfying result. However the terminal velocities while being within the same order ($4L.T^{-1}$ against $12L.T^{-1}$) still differ. We can also observe a diffusion around the sphere constrained with the H1/viscous penalty. This could be explained by the fact that no specific treatment regarding the interface is used when computing the viscous part of the momentum equation of the penalized problem. Meanwhile the Darcy penalty probably requires corrections regarding the physical parameters and external forces to obtain a coherent coupling between the Newton laws and the fluid problem.

### 3.2 A Rigid Rod in a Lid–Driven Cavity

To demonstrate the marker strategy with a non–spherical particle, we place a rigid rod in the domain $\Omega = [0, 1]^3$ with the boundary conditions of a lid–driven cavity problem. On the side $\{(x, y, z) \in \Gamma, z = 1\}$ of $\Omega$ we set $\boldsymbol{u}(t, \boldsymbol{x}) = 1$. The rigid rod is defined with the density $\rho_s = 0.8$, a length $l = 0.1$ and width $w = 0.02$. For the fluid we use $\mu_f = 1.0$. We neglect the gravity and leave the boundary conditions to establish the flow. We use the spatial step $h = 1/70$ and the same time step as the previous test. We take $\mu_s = 10^4$ to penalize the solid (Fig. 4).

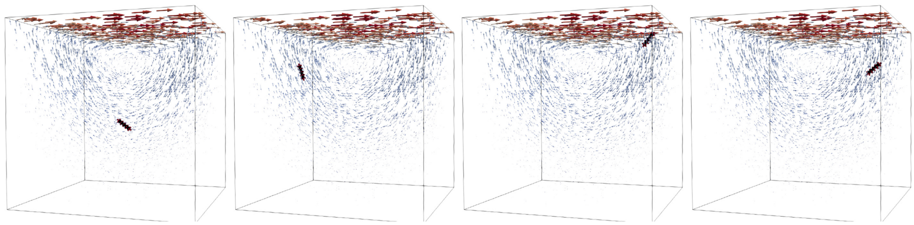

**Fig. 4.** State of the problem at times $t = 2.25$, $t = 4, 25$, $t = 6.0$, $t = 6.75$

Despite the rather coarse mesh and the thin rod used in this test, the particle properly follows the flow and rotates appropriately, while remaining rigid. The markers seem to handle correctly the decomposition of a complex particle using sub–spheres from the collision strategy.

## 4 Concluding Remarks

We were able to study and compare the L2-penalty and the H1-penalty methods in the context of particulate flows. As far as we know, comparative studies between those two methods do not exist for such situations. Therefore, this work can be considered as a novel short progress in this direction. The numerical tests were overall satisfying and allowed us to take a step further in validating our code. However more work is required regarding the calibration of the Darcy penalty problem and the sharpness of the interface with the viscous–penalized problem to help with the comparison of the methods and the global observations.

## References

1. Glowinski, R., Pan, T.-W., Hesla, T.I., Joseph, D.D.: A distributed Lagrange multiplier/fictitious domain method for particulate flows. Int. J. Multiph. Flow **25**, 755–794 (1999)
2. Angot, P., Bruneau, C.-H., Fabrie, P.: A penalization method to take into account obstacles in incompressible viscous flows. Numer. Math. **81**, 497–520 (1999)

3. Khadra, K., Angot, P., Parneix, S., Caltagirone, J.-P.: Fictitious domain approach for numerical modelling of Navier-Stokes equations. Int. J. Numer. Methods Fluids **34**, 651–684 (2000)
4. Carbou, G., Fabrie, P.: Boundary layer for a penalization method for viscous incompressible flow. Int. Adv. Differ. Equ. **8**(12), 1453–1480 (2003)
5. Guermond, J.L., Minev, P., Shen, J.: An overview of projection methods for incompressible flows. Comput. Methods Appl. Mech. Eng. **195**, 6011–6045 (2006)
6. Févrière, C., Laminie, J., Poullet, P., Angot, P.: On the penalty-projection method for the Navier-Stokes equations with the MAC mesh. J. Comput. Appl. Math. **226**, 228–245 (2009)
7. Angot, P., Caltagirone, J.-P., Fabrie, P.: A kinematic vector penalty-projection method for incompressible flow with variable density. Comptes Rendus Mathématique **354**(11), 1124–1131 (2016)
8. Faure, S., Martin, S., Maury, B., Takahashi, T.: Towards the simulation of dense suspensions: a numerical tool. ESAIM Proc. **28**, 55–79 (2009)